ORIGINAL PAPER

Biophysical Studies on the Interactions of a Classic Mitochondrial Uncoupler with Bovine Serum Albumin by Spectroscopic, Isothermal Titration Calorimetric and Molecular Modeling Methods

Yue Zhang · Jia-Han Li · Yu-Shu Ge · Xiao-Rong Liu · Feng-Lei Jiang · Yi Liu

Abstract The interaction between a classic uncoupler (2,4-dinitrophenol, DNP) and bovine serum albumin (BSA) was investigated by fluorescence spectroscopy under the physiological conditions. The fluorescence quenching constants were calculated by the Stern-Volmer equation, and based upon the temperature dependence of quenching constants, it was proved that DNP caused a static quenching of the intrinsic fluorescence of BSA. Owing to the static quenching mechanism, different associative binding constants at various temperatures were determined and thus the thermodynamic parameters, namely enthalpy ($\Delta H = -21.12$ kJ mol^{-1}) and entropy changes ($\Delta S = 23.51$ J mol^{-1} K^{-1}) could be calculated based on the binding constants. Moreover, the enthalpy and entropy changes are consistent with the "Enthalpy-Entropy Compensation" equation obtained from our previous work. The negative enthalpy and positive entropy indicated that the electrostatic interactions played a major role in DNP-BSA binding process. Site marker competitive displacement experiments were carried out by using fluorescence and isothermal titration calorimetry (ITC) methods. These results showed that DNP bound with high affinity to Sudlow's site I (subdomain IIA) of BSA. The distance ($r = 3.78$ nm) between donor (BSA) and acceptor (DNP) was obtained according to the mechanism of fluorescence resonance energy transfer (FRET). Furthermore, the results of synchronous fluorescence and circular dichroism (CD) spectroscopic studies indicated that the microenvironment and the secondary conformation of BSA were altered. The above results were supported by theoretical molecular modeling methods.

Introduction

Serum albumins are the major soluble protein in the circulatory system and have many physiological functions. This protein not only has a significant contribution to transport unesterified fatty acids, but also has the capability to bind with an extraordinarily diverse range of metabolites, drugs, dyes and organic compounds [1, 2]. Since the overall distribution, metabolism and efficacy of many drugs in the body are correlated with their affinities towards serum albumin [1], the investigation of compound-albumin binding becomes important in the rational drug-design process. The information on the interaction of serum albumins with drugs can allow us to better understand the absorption and distribution of drugs in vivo. Bovine serum albumin (BSA) has been one of the most extensively studied among this group of proteins, particularly because of its structural homology with human serum albumin (HSA). BSA has two tryptophan residues (Trp-134 and Trp-212) that exhibit intrinsic fluorescence. Specifically, Trp-134 is located at the surface of the molecule while Trp-212 is located within a hydrophobic binding pocket of the protein [3]. Since the intrinsic fluorescence of BSA is usually quenched upon binding to some drugs, the fluorescence spectroscopy is sensitive and relatively easy to provide useful information

Y. Zhang · J.-H. Li · Y.-S. Ge · X.-R. Liu · F.-L. Jiang · Y. Liu (✉)
State Key Laboratory of Virology & Key Laboratory of Analytical Chemistry for Biology and Medicine (Ministry of Education) & College of Chemistry and Molecular Sciences, Wuhan University, Wuhan 430072, People's Repulic of China
e-mail: prof.liuyi@263.net

for the structural features that determine the therapeutic effectiveness of drugs [4, 5]. Fluorescence quenching measurements can reveal the accessibility of quenchers to the fluorophore groups of BSA, help understand the binding mechanism of albumins with drugs, and provide clues on the essence of the binding phenomenon [6]. In the past few years, our group has been focusing on the interactions of serum albumin with pharmaceutical drugs in order to understand the pharmacokinetics and pharmacodynamic properties [4, 5, 7–22], with dyes to find out how bio-probes behave in the circumstance of proteins [23–26], and with quantum dots to shine light on the influence of nanomaterials on environment [27].

Since mitochondria can produce most of the energy in cells and play a crucial role in the cell growth and death, our group has been continuing research on the effect of various metal ions, drugs and pre-drugs on mitochondria by microcalorimetric and microscopic methods [28, 29]. Among the bioactive molecules, the mitochondrial uncouplers have attracted much attention. They are protonophoric compounds that effectively allow protons to "leak" back into the mitochondrial matrix with a consequent reduction in mitochondrial membrane potential. Previously, researches have focused on the mechanism of uncoupling of oxidative phosphorylation [30–33]. Among the uncouplers, 2,4-dinitrophenol (DNP; Scheme 1), a cellular metabolic poison, is a classic mitochondrial uncoupler and has been studied the most [34]. DNP is often used in biochemistry to explore the bioenergetics of chemiosmotic and other membrane transport processes, but the nature of its interaction with serum albumin has not been investigated. As previously reported, the action of uncouplers is mediated by some proteins and the uncouplers were postulated to be involved in the cellular defense mechanism preventing the formation of superoxide [35]. Therefore, it is of great interest to study the binding of DNP with BSA in order to elucidate how DNP interacts with BSA, the most abundant protein in blood and the most

important transporter for the endogenous and exogenous molecules, and to shine light on its bioactivities.

Herein, the interactions between DNP and BSA were characterized by fluorescence quenching spectroscopy which determined the quenching mechanism and thermodynamic parameters such as enthalpy change, entropy change and free energy change. Circular dichroism (CD) and synchronous fluorescence spectroscopic studies have provided insight into the structural influence of DNP on BSA. The site marker competitive displacement experiments by fluorescence spectroscopic method showed DNP bound to the Sudlow's site I (subdomain IIA), which agreed well with the conclusion obtained from isothermal titration calorimetric studies. To the best of our knowledge, this is the first report that determines the binding site by this method. Finally, comprehensive binding mechanism was theoretically studied by molecular modeling method which proposed a description of the binding behavior.

Experimental Section

Materials

DNP and bovine serum albumin (BSA) were purchased from Sigma-Aldrich and used as received. The molecular weight of BSA was assumed to be 66,500 g mol^{-1}. Its stock solution was prepared in phosphate buffered saline (PBS, 0.02 M of phosphate, 0.10 M of NaCl, pH=7.4) and kept in the dark at 277 K. All other reagents were of analytical reagent grade and all solutions were prepared with double-distilled water.

Fluorescence and UV-vis Absorption Measurements

The fluorescence spectra were recorded on a LS-55 Spectrofluorimeter (Perkin-Elmer) with a thermostat for measurement at four temperatures (298, 304, 310 and 316 K). The protein concentration in all experiments was made with 1.0×10^{-5} mol L^{-1}. The excitation wavelength was set to 285 nm and the emission spectra were recorded in the range from 300 to 450 nm. Control samples corresponding to the buffer were subtracted to correct the background. The data were analyzed by the Stern-Volmer or modified Stern-Volmer equation.

The UV-vis absorption spectra were recorded at room temperature on a UNICO 4802 double beam spectrophotometer equipped with 1.0 cm quartz cells.

Circular Dichroism Measurement

CD spectra were recorded on an Applied Photophysics Chirascan instrument at 298 K under constant nitrogen flush. A cell with a 0.1 cm of path length was used for data collection recorded between 200 and 260 nm with an interval of 1 nm.
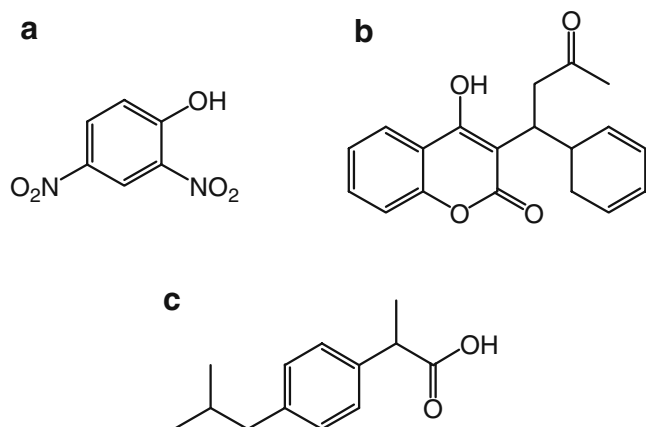
Scheme 1 Molecular structure of **a** 2,4-dinitrophenol (DNP), **b** warfarin and **c** ibuprofen

Isothermal Titration Calorimetry (ITC) Measurement

The isothermal titration calorimetric experiments were carried out on a nano-ITC^{2G} isothermal titration calorimeter (TA Instrument Corp., USA). The microcalorimeter consists of a reference cell and a sample cell of 1 mL in volume, with both cells insulated by an adiabatic shield. All solutions were thoroughly degassed before use by stirring under vacuum. The sample cell was loaded in turn with BSA solution (1.0×10^{-4} mol L^{-1}), BSA-warfarin complex and BSA-ibuprofen complex, respectively. A 100 μL of antopipet was filled with the DNP solution (3.0×10^{-3} mol L^{-1}) and its stirring speed was fixed at 300 rpm. Injections were started when baseline stability had been achieved. DNP was titrated into the sample cell as a sequence of 20 injections of 5 μL aliquots while the temperature of the system was maintained at 298 K. The time delay (allowing for equilibration) between successive injections was 10 min. To correct the heat effect due to mixing and dilution, control experiment was done in which DNP was injected into the buffer solution without BSA.

Molecular Modeling

The structure of DNP was generated with sybyl8.1 package. The molecule was optimized using Tripos Force Field after been charged. The total energy of the final molecule was 5.445 kcals mol^{-1}. The crystal structure of bovine serum albumin was modeled with Modeller_9v7. The sequence of the protein was obtained from NCBI database (http://www.ncbi.nlm.nih.gov/Database/; ID: CAA76847). The Basic Local Alignment Search Tool (BLAST) of the sequence of BSA and HSA (PDB database) had given the highest homogeneous identity crystal structure of HSA (pdb entry: 1AO6). The model structure of BSA used here was according to this crystal structure. The protein structure was analyzed with Sybyl8.1 software, and all the side chains were repaired whilst the bumps were fixed when necessary. Additionally, H atoms were added. The biopolymer was charged using AMBER7 FF99 method. This structure was applied in the Surflex Dock program which was used to compute the docking mode of the DNP-BSA complex. The location of DNP in BSA was defined with residues.

Results and Discussion

Binding Constant

Prior to studying the binding constants between DNP and BSA, the quenching mechanism has been determined by fluorescence quenching spectroscopy. The fluorescence spectra of BSA (λ_{ex}=285 nm) in the presence of different concentrations of DNP are obtained at pH 7.4 and 298 K (Fig. 1). The fluorescence intensity of BSA decreases regularly with increasing concentration of DNP. When the molar ratio between DNP and BSA comes to 1:1, the fluorescence intensity is reduced to 45% from its original intensity. The emission maxima (λ_{em}) is near 350 nm and is slightly blue-shifted (by 2 nm) when in the presence of DNP. This result implies that the addition of DNP can slightly increase the hydrophobicity (or decrease the polarity) of the region surrounding the tryptophan in BSA [36].

The fluorescence quenching mechanism can be classified into two categories, the so-called "dynamic and static quenching", which can be distinguished by their different dependence on temperature and viscosity. Since higher temperatures lead to larger diffusion coefficients, the dynamic quenching constants are expected to become larger with increasing temperature. In contrast, increased temperature is likely to result in decreased stability of complexes, and thus smaller value of the static quenching constant [7]. By this way, the type of interactions can be identified. Fluorescence quenching can be described by the Stern-Volmer equation as follow [37]:

$$\frac{F_0}{F} = 1 + K_{SV}[Q] = 1 + k_q \tau_0 [Q] \qquad (1)$$

where F_0 and F are the fluorescence intensities in the absence and presence of a quencher, respectively, $[Q]$ is the concentration of the quencher, K_{SV} is the Stern-Volmer quenching constant, k_q is the biomolecular quenching constant, and τ_0 is the fluorescence lifetime in the absence of quencher. Equation (1) is applied to determine K_{SV} by
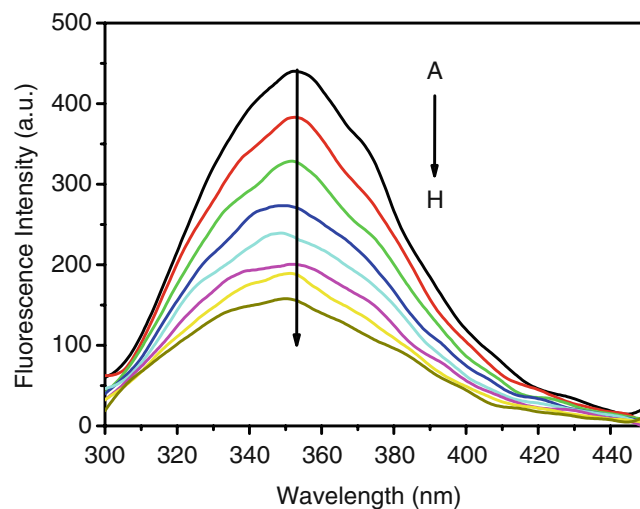
Fig. 1 Effect of the increasing concentrations of DNP on the fluorescence spectrum of BSA (T=298 K, pH=7.4, λ_{ex}=285 nm). c(BSA)=1.0×10^{-5} mol L^{-1}; c(DNP)/(10^{-5} mol L^{-1}) (A–H): 0, 0.2, 0.4, 0.6, 0.8, 1.0, 1.2 and 1.4

linear regression of the plot of F_0/F against $[Q]$. In order to interpret the possible quenching mechanism, the dependence of the quenching constant (K_{SV}) with the temperature is studied. Table 1 shows that the K_{SV} is inversely correlated with the temperature (298 K, 304 K, 310 K and 316 K), which indicates that the probable quenching process of BSA interacting with DNP is a static rather than a dynamic quenching.

As for the static quenching procedure, the data can be analyzed according to the modified Stern-Volmer equation [37]:

$$\frac{F_0}{\Delta F} = \frac{F_0}{F_0 - F} = \frac{1}{f_a K_a} \frac{1}{[Q]} + \frac{1}{f_a} \quad (2)$$

In this case, ΔF is the difference of fluorescence intensity in the absence and presence of the quencher at the concentration $[Q]$, f_a is the fraction of accessible fluorescence and K_a is the effective quenching constant for the accessible fluorophores, which can be considered as the associative binding constants for the donor-acceptor system. The dependence of $F_0/\Delta F$ on the reciprocal value of the quencher concentration ($1/[Q]$) is linear with slope equal to the value of $1/f_a K_a$. The value of $1/f_a$ is fixed on the ordinate. The constant K_a is a ratio of the ordinate $1/f_a$ over the slope $1/f_a K_a$. The corresponding results at different temperatures are shown in Fig. 2 and Table 2. It is clear that the binding constants K_a slightly decreases with increasing temperature. The K_a at 298 K is 8.673×10^4 L mol^{-1} in the range from 10^4 to 10^6, which is the suitable range for association and dissociation in drug-protein systems, in consideration of favorable transportation of drugs with binding constant in this range.

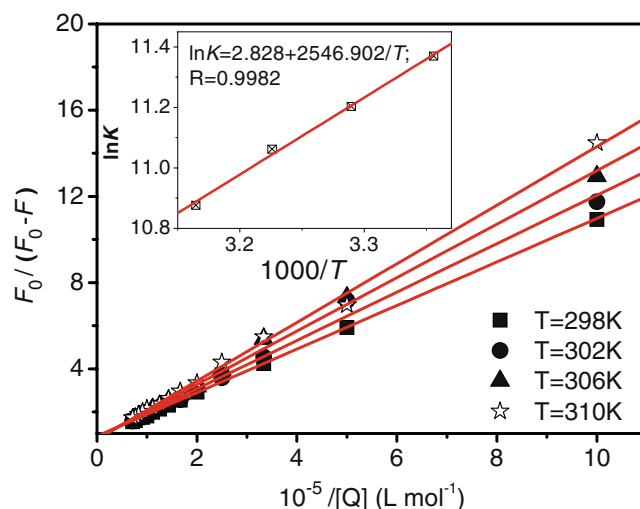Thermodynamic Parameters and Interaction Forces

Generally, the interaction forces between a ligand and protein may include hydrophobic interactions, electrostatic attractions and repulsions, van der Waals interactions, hydrogen-bonding forces, etc [38, 39]. In order to figure out the nature of the interactions between DNP and BSA,

Fig. 2 Modified Stern-Volmer plots of fluorescence quenching of BSA caused by the addition of DNP at 298 K, 304 K, 310 K and 316 K. The inset is the van't Hoff plot in PBS, pH=7.40

the thermodynamic parameters are calculated according to the van't Hoff equation [40]:

$$\ln K_a = -\frac{\Delta H}{RT} + \frac{\Delta S}{R} \quad (3)$$

where R is the gas constant, ΔH is the enthalpy change and ΔS is the entropy change. And the free energy change (ΔG) can be calculated by the following equation:

$$\Delta G = \Delta H - T \Delta S \quad (4)$$

A plot of $\ln K_a$ versus $1/T$ (inset in Fig. 2) enables the determination of ΔH and ΔS for the binding at different temperatures (Table 2). Considering the enthalpy change and entropy change obtained in our previous works [4, 5, 7–27], there is a linear relationship between ΔH and ΔS, which is called the "Enthalpy-Entropy Compensation" and expressed as the following equation:

$$\Delta H(\text{J mol}^{-1}) = -2.678 \times 10^4$$
$$+ 299.788 \Delta S(\text{J mol}^{-1}\text{K}^{-1}), \ R = 0.9796 \quad (5)$$

When ΔS is 23.51 J mol^{-1} K^{-1} (this work), ΔH=19.73 KJ mol^{-1} with the deviation of 6.6% from the experimental value, showing the good applicability of this equation (Fig. 3).

In Fig. 3, four zones can be depicted: (I) enthalpically driven; (II) both enthalpically and entropically driven; (III) entropically driven; (IV) no reaction will occur in this area. Consequently, this reaction is both enthalpically and entropically driven. The negative enthalpy (ΔH) and positive entropy (ΔS) values for the interaction between DNP and BSA indicate that the electrostatic interactions

Table 1 Stern-Volmer quenching constants (K_{SV}) of the DNP-BSA complex at different temperatures

pH	T(K)	$10^{-5}K_{SV}$ (L mol^{-1})	R[a]	S.D.[b]
7.40	298	1.267	0.994	0.071
	304	1.205	0.996	0.061
	310	1.147	0.996	0.057
	316	0.992	0.997	0.042

[a] The correlation coefficient

[b] The standard deviation for the K_{SV} values

Table 2 Binding constant (K_a) and thermodynamic parameters of DNP-BSA complex

T (K)	$10^{-4}K_a$ (L mol^{-1})	R^a	ΔG (kJ mol^{-1})	ΔH (kJ mol^{-1})	ΔS (J mol^{-1} K^{-1})	R^b	S.D.^{c}
298	8.673	0.999	−28.12	−21.12	23.51	0.998	0.016
304	7.342	0.996	−28.27				
310	6.379	0.998	−28.41				
316	5.291	0.998	−28.55				

^{a} The correlation coefficient for K_a

^{b} The correlation coefficient for the van't Hoff plot

^{c} The standard deviation for the van't Hoff plot

play a major role in the binding process [38]. Additionally, the negative free energy change (ΔG) implies that the binding process is spontaneous. In cells, the weak acid DNP acts as a proton ionophore, an agent that can shuttle protons (hydrogen ions) across biological membranes. Although albumin carries a net negative charge at physiological pH, it also has positively charged pockets to bind anionic ligands [41, 42]. In aqueous solutions, free DNP anion may collide with the positively charged site and thereafter electrostatic interactions occur.

Binding Site

For static quenching, the fluorescence intensity can also be used to analyze the apparent binding constant (K_b) and the number of binding sites (n) using Eq. (6) when small molecules independently bind to a set of equivalent sites on a macromolecule [43]:

$$\log \frac{F_0 - F}{F} = \log K_b + n \log[Q] \qquad (6)$$
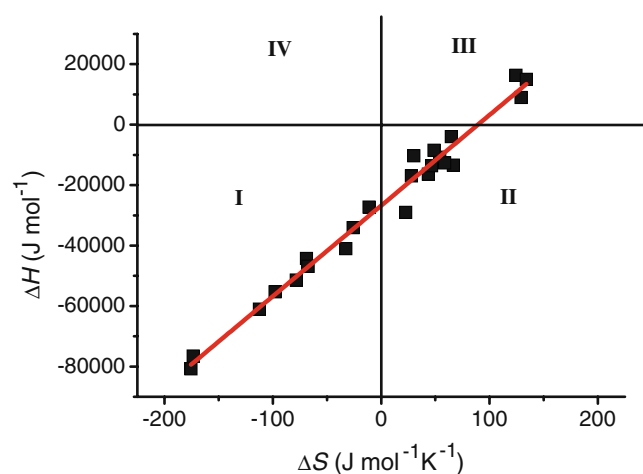
Fig. 3 Enthalpy-entropy compensation. (I) enthalpically driven; (II) both enthalpically and entropically driven; (III) entropically driven; (IV) no reaction will occur in this area. The data points are collected from Ref. [4, 5, 7–27]

The number of binding sites of DNP–BSA system extracted from Eq. (6) is approximately 1. The result suggests that there is only one type of binding site for DNP on BSA. BSA is a heart-shaped helical monomer composed of three structurally homologous and predominantly helical domains (I, II and III), each containing two subdomains (A and B) [9]. The crystal structure analyses also indicate that the principal regions of ligand-binding sites in albumin are located in hydrophobic cavities in subdomains IIA and IIIA which are also named site I and II, respectively, according to Sudlow's nomenclature [44].

To identify the binding site of DNP on BSA, site marker competitive displacement experiments are carried out with the help of probes (warfarin and ibuprofen; Scheme 1) that specifically bind to a known site or region on BSA. Specifically, warfarin binds to Sudlow's site I whereas ibuprofen prefers Sudlow's site II [2]. The DNP-binding site can be deduced by monitoring the changes in the fluorescence spectroscopy of site marker-bound BSA upon addition of DNP. In this experiment, DNP was gradually added to the co-solution of BSA and site marker with the same concentrations (1.0×10^{-5} mol L^{-1}). To facilitate the comparison of the influence of warfarin and ibuprofen on the binding of DNP to BSA, the binding constants in the presence of site markers are analyzed using the modified Stern-Volmer equation (Eq. (2)) (Fig. 4). The binding constant (K_a) of the DNP–BSA complex in the presence of warfarin decreases from 8.67×10^4 to 4.66×10^4 L mol^{-1} when DNP is added, whereas the K_a in the presence of ibuprofen is not affected when titrated by DNP (8.67×10^4 vs 8.06×10^4 L mol^{-1}). Noteworthy, the binding constant with warfarin is just 53% of that without warfarin, whereas there is almost no influence in the presence of ibuprofen, indicating the competitive displacement of warfarin rather than ibuprofen. It can be deduced that DNP binds with high affinity to Sudlow's site I (subdomain IIA) in BSA.

In order to support the conclusion, the site marker competitive displacement experiments were also carried out using the isothermal titration calorimetry (ITC). ITC is a convenient approach for the study of biomolecular interactions since enthalpy changes will occur during any
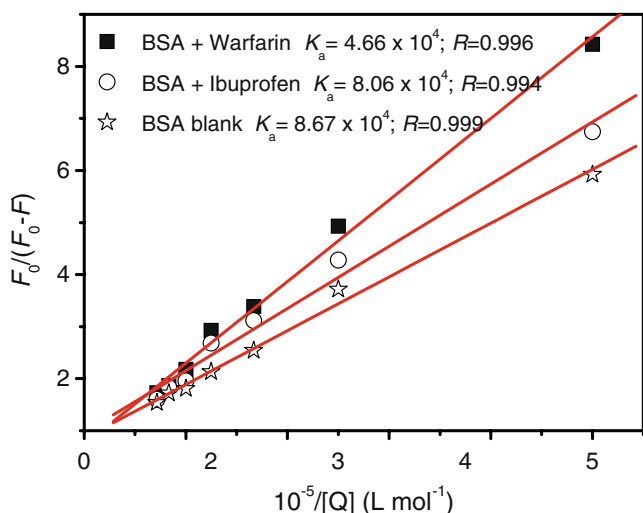
Fig. 4 Site marker competitive displacement experiments of DNP–BSA system in the presence of warfarin and ibuprofen, respectively

interaction that leads to the formation of a complex. It is one of the only two methods that are able to directly determine the interaction enthalpy (the other one is differential scanning calorimetry, DSC) [45, 46]. The main advantage of ITC is its ability to characterize any type of interaction and provide the values of complex stoichiometry (n), stability constant (K), and enthalpy change (ΔH) in one experiment. Although it has some limitations related to the order of magnitude of the interaction measured and the stability constant which cannot be measured directly [47, 48], the calorimetric titration plots can directly help us understand the binding site of DNP binding on BSA. Each peak in the binding isotherm (Fig. 5) represents a single injection of DNP solution. The positive deviations of the heat signal from the baseline on addition of DNP indicate that heat is evolved. It is apparent from Fig. 5a that the interaction between DNP and BSA is exothermic and that, from the shape of the binding isotherms, the actual binding saturation is not reached within the experiment. As shown in Fig. 5b, the titration experiment of DNP into the warfarin-BSA system demonstrates that the exothermicity is remarkably lower than that without warfarin (c.a. 75% decrease). In other words, the exothermic heat pulses caused by the binding of DNP to BSA are reduced in the presence of warfarin. This observation indicates that the binding of DNP to BSA is affected by the presence of warfarin. However, similar isotherms have been observed for the binding of DNP to BSA in the absence (Fig. 5a) and presence (Fig. 5c) of ibuprofen. This proves that site II marker does not interfere with the usual binding site of DNP on BSA. Our observations by ITC confirm the binding site at Sudlow's site I and are consistent with the conclusion deduced by fluorescence quenching spectroscopic methods above.
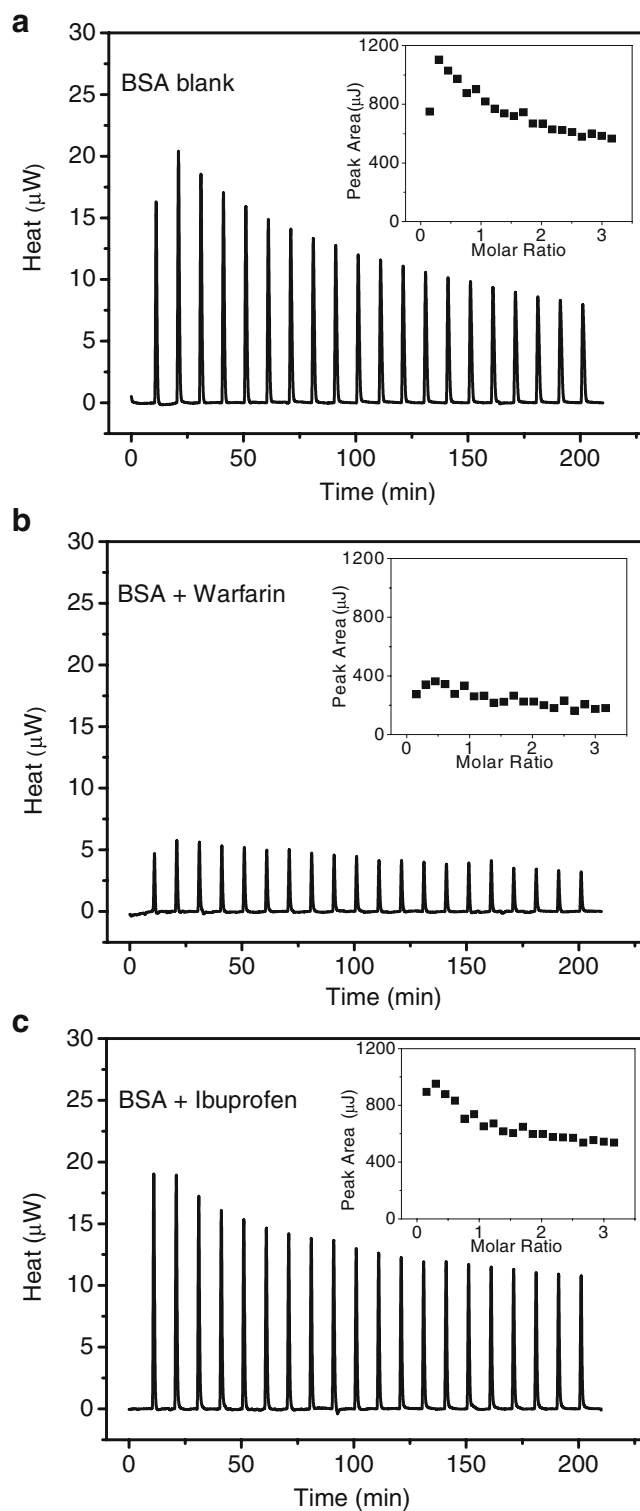
Fig. 5 Titration of DNP into the solution of BSA measured by ITC. The signal (heat) for the titration of 0.1 mM of BSA with 3 mM of DNP in the absence of site marker (**a**), in the presence of 0.1 mM of warfarin (**b**), and 0.1 mM of ibuprofen (**c**) at pH 7.4 and 298 K, shows the calorimetric response when successive injections of DNP are added to the sample cell. Inset panel: integrated heat profile of the calorimetric titration

Binding Distance

Fluorescence resonance energy transfer (FRET) is usually applied to determine the mean distance between amino acid residues (the donor) and the bound drugs (the acceptor) [49]. Using FRET, the efficiency of energy transfer (E) can be expressed by the following equation [37]:

$$E = 1 - \frac{F}{F_0} = \frac{R_0^6}{R_0^6 + r^6} \tag{7}$$

where r is the average distances between a donor and an acceptor, and R_0 is the critical distance at which the transfer efficiency is 50%.

$$R_0^6 = 8.79 \times 10^{-25} K^2 n^{-4} \phi J \tag{8}$$

where K^2 is the orientation factor of the dipole and $K^2 = 2/3$ for random orientation in fluid solution, n is the refracted index of the medium, Φ is the fluorescence quantum yield of the donor, and J is the overlap integral of the fluorescence emission spectrum of the donor and the absorption spectrum of the receptor (Fig. 6).

$$J = \frac{\int_0^\infty F(\lambda)\varepsilon(\lambda)\lambda^4 d\lambda}{\int_0^\infty F(\lambda)d\lambda} \tag{9}$$

where $F(\lambda)$ is the fluorescence intensity of the donor at wavelength λ, $\varepsilon(\lambda)$ is the molar absorption coefficient of the acceptor at wavelength λ. In the present case, $n=1.36$, $\Phi=0.15$ [50]. Using Eqs. (7), (8), (9), we obtain that $J=1.22\times10^{-14}$ cm^3 L mol^{-1}, $R_0=3.88$ nm, $E=0.53$ and $r=3.78$ nm. R_0 and r are in the 2–8 nm scale, and $0.5\,R_0 < r < 1.5\,R_0$, indicating that the energy transfer from BSA to DNP occurs with a large probability [51].
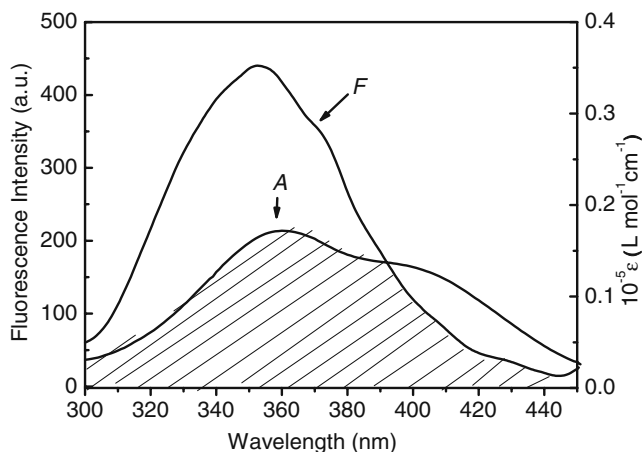
Fig. 6 Spectral overlap of the absorption spectrum of DNP (curve A) with the fluorescence spectrum of BSA (curve F) at 298 K. c(BSA) = c(DNP)=1.0×10^{-5} mol L^{-1}

Conformational Change

Synchronous Fluorescence Spectroscopy

Synchronous fluorescence spectroscopy introduced by Llody has been used to study the microenvironment of amino acid residues by measuring the shift of emission maxima [52]. The spectra were obtained by simultaneously scanning the excitation and emission monochromators. When $\Delta\lambda$ between excitation wavelength and emission wavelength is set as 60 and 15 nm, the synchronous fluorescence offers characteristic information of tryptophan residues and tyrosine residues, respectively [53]. Synchronous fluorescence spectra of BSA upon addition of DNP are shown in Fig. 7. The emission maxima of both tryptophan and tyrosine residues are blue-shifted for 4 nm
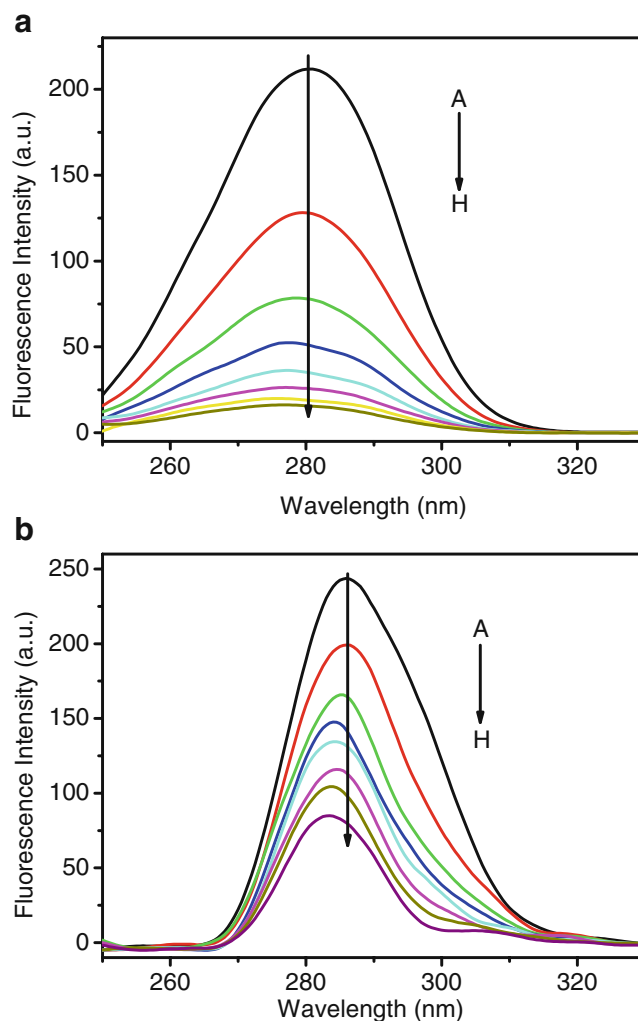
Fig. 7 Synchronous fluorescence spectrum of BSA in the presence of different concentrations of DNP. (A) $\Delta\lambda=60$ nm, c(BSA)=1.0×10^{-5} mol L^{-1}, c(DNP)/(10^{-5} mol L^{-1}) (A–H): 0, 0.5, 1, 1.5, 2, 2.5, 3 and 3.5; (B) $\Delta\lambda=15$ nm, c(BSA)=1.0×10^{-5} mol L^{-1}, c(DNP)/ (10^{-5} mol L^{-1}) (A–H): 0, 0.5, 1, 1.5, 2, 3, 4 and 5
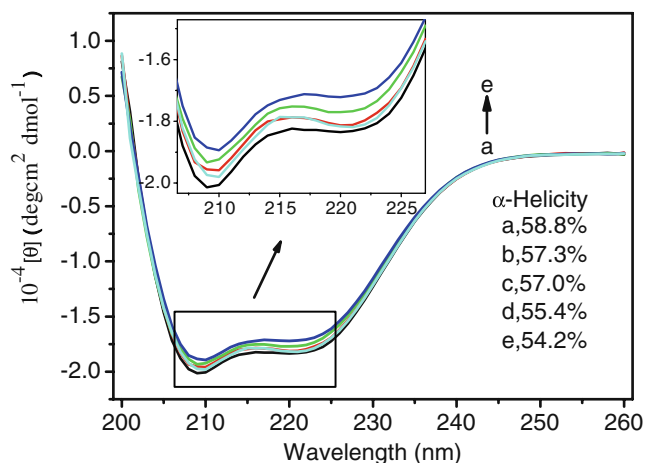
Fig. 8 Circular dichroism spectra of BSA in the absence and presence of DNP. The molar ratios of DNP to BSA are from a to e, 0:1, 5:1, 10:1, 20:1 and 40:1

and 2 nm, respectively, at the investigated concentration range. The blue-shift effect indicates that both the microenvironment of tryptophan and tyrosine residues are altered, which suggests a more hydrophobic (or less polar) microenvironment surrounding the amino acid residues.

Circular Dichroism (CD)

To prove the possible influence of DNP binding action on the secondary structure of BSA, its CD spectra were measured when DNP was added. This method has been widely used for studying the conformation and conformational change of proteins and polypeptides in solution [54]. The CD spectra of BSA exhibit a typical shape of α-helix rich secondary structure (two negative bands at approximately 208 and 222 nm). The CD results are expressed in terms of mean residue ellipticity (MRE) in deg cm^2 dmol^{-1} according to the following equation:

$$MRE = \frac{observed CD(m \deg)}{c_p nl \times 10} \quad (10)$$

where c_p is the molar concentration of the protein, n is the number of amino acid residues and l is the path length. The

α-helical contents of free and combined BSA are calculated from MRE values at 208 nm using the equation [55]:

$$\alpha - helix(\%) = \frac{-MRE_{208} - 4000}{33000 - 4000} \times 100\% \quad (11)$$

where MRE_{208} is the observed MRE value at 208 nm. Figure 8 shows the far-UV CD spectra of BSA in the absence and presence of DNP at pH 7.4 and room temperature. In order to quantify the different types of content of secondary structures, the CD spectra have been analyzed using the algorithm SELCON3 (Table 3), with 43 model proteins with known precise secondary structures used as the reference set [56, 57]. BSA shows a decrease in α-helical structure and an increase in β-sheet structure in the presence of DNP, confirming the interaction between DNP and BSA. A decrease in α-helical from 58.8 to 54.2% demonstrates the loss of the biological activity of BSA upon interaction with higher concentration of DNP. DNP is bound to the amino acid residues of the main polypeptide chain of BSA and the interaction destroys the original hydrogen-bonding networks [58]. This conclusion is consistent with the results of synchronous fluorescence spectroscopic study that the microenvironment and secondary structure undergo some changes but to some extent.

Molecular Modeling

In order to confirm the precise binding site on BSA, molecular modeling is employed to simulate the binding mode between DNP and BSA. The crystallographic analyses of HSA have revealed that HSA contains three homologous domains (I, II, and III), each of which has two subdomains (A and B) possessing cylindrical structures. The principal regions of HSA for drug-binding are located in hydrophobic cavities in subdomains IIA and IIIA (sudlow's site I and II, respectively). We consider BSA has the equivalent binding sites with HSA, since the sequence of BSA and HSA share more than 80% homology in their amino acid sequence. The residues in the bovine sequence which are not the same as those in the human template crystal structure (PDB code: 1AO6) are not included in the model [59]. The result suggests that DNP
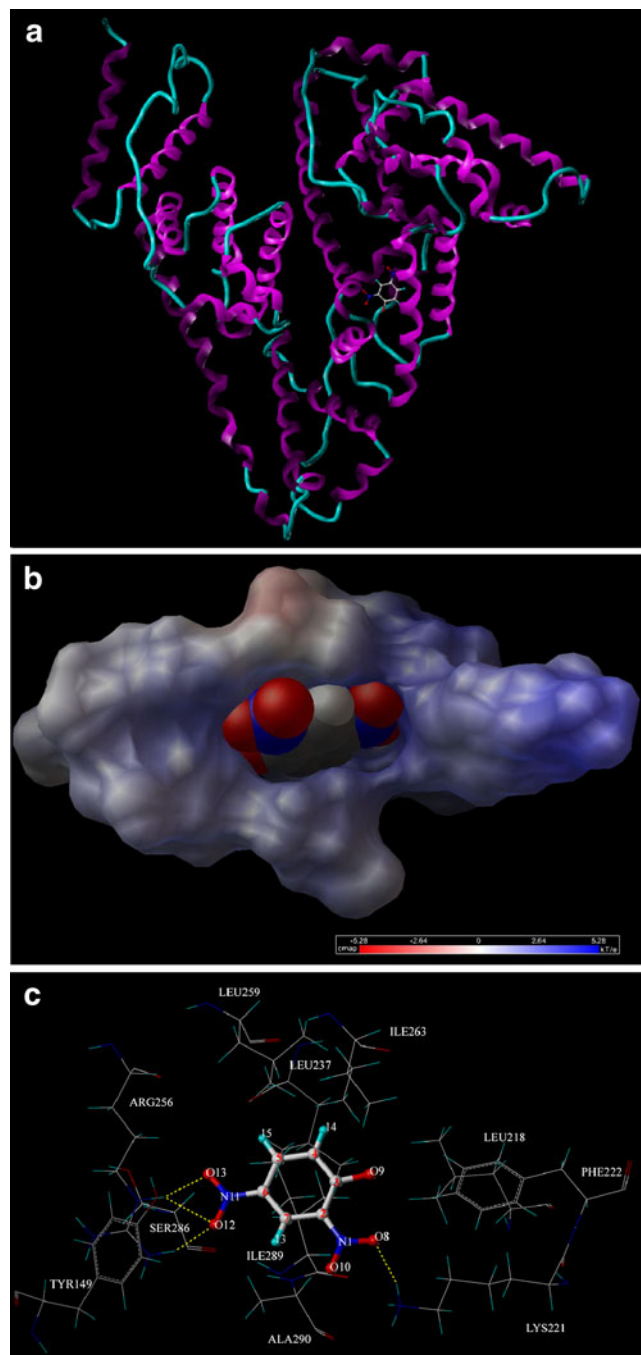
Table 3 Secondary structure of DNP-bound BSA determined by SELCON3

Molar ratio [DNP]:[BSA]	α-Helix (%) [a]		β-Sheet (%)		Turn (%)	Unordered (%)
	H(r)	H(d)	S(r)	S(d)		
0:1	38.3	20.5	2.9	3.5	16.1	20.4
5:1	37.2	20.1	3.2	3.6	16.3	20.8
10:1	37.0	20.0	3.2	3.5	16.6	21.3
20:1	35.8	19.6	4.0	4.0	16.6	22.3
40:1	34.8	19.4	4.1	4.2	17.5	22.7

[a] "*r*" and "*d*" represent "ordered" and "disordered", respectively

is located within the binding pocket of subdomain IIA which is consistent with the results obtained by site marker competitive displacement experiments and ITC measurements (Fig. 9a). It can be seen from Fig. 9b that electrostatic forces would be the driving factor in the

interaction. Figure 9c exhibits there are several amino acid residues with polar chains (Ser286, Arg256, Trp149 and Lys221) in the vicinity of DNP. The hydrogen-bonding forces also contribute to stabilizing the DNP–BSA complex as shown with dashed lines. The results agree well with the experimental. The distances of residues lying within 5 Å from any of the atoms of DNP are listed in Table 4 and it confirms that the binding distance between DNP and BSA is c.a. 3.78 nm as the experimental data aforementioned.

Conclusion

We have studied the interaction of DNP with BSA in a systematic manner including fluorescence and circular dichroism spectroscopy as well as isothermal titration calorimetric methods. The fluorescence quenching spectroscopy suggests a static quenching mechanism with a binding constant of $\sim 10^5$, in the range suitable for drug transportation. The thermodynamic parameters are obtained based on the binding constants at different temperatures and are consistent with the "Enthalpy-Entropy Compensation" equation, the equation summarized from our previous work. The negative enthalpy and positive entropy imply that electrostatic force contributes greatly to the DNP-BSA complex. Site marker competitive displacement experiments by fluorescence spectroscopy demonstrate that the binding site is the Sudlow's site I (subdomain IIA) and the result is confirmed by isothermal titration calorimetric studies, which are conducted for the first time to differentiate the binding sites of serum albumins. Both the synchronous fluorescence and circular dichroism spectroscopic studies indicate that the microenvironment and secondary structure of BSA are altered to some degree. Finally, the above conclusions are corroborated by molecular modeling calculations. This work

Fig. 9 a The binding mode of DNP with BSA. b The surface electrostatic potential map of BSA with DNP (from red to blue: negatively charged regions to positively charged ones). c Only those residues that are located around DNP are presented. The residues of BSA are represented by solid lines and DNP with ball and stick model for clarity. The hydrogen bonds between DNP and BSA are presented with dashed lines

Table 4 The distances between the DNP atoms and the atoms of residues obtained by molecular modeling

Atom of the residue	Atom of DNP	Distance (Å)
ALA 290 C3	O 10	3.22
ILE 263 C3	C 4	3.32
ILE 289 C3	C 5	4.22
SER 286 C3	O 13	4.31
LEU 237 C3	C 6	4.13
ARG 256 Np13	O 12	2.95
TYR 149 O3	O 12	3.83
LEU 259 C3	C 5	3.28
PHE 222 Car	O 9	4.22
LEU 218 C3	O 8	3.20
LYS 221 N4	O 3	3.02

Residues lying within 5 Å from any of the atoms of DNP are listed

is expected to provide valuable information for the transportation and distribution of DNP in vivo, and be helpful in clarifying the biological effects and dynamics of DNP.

References

1. Wesley RH (1996) Binding and transport of aluminum by serum proteins. Coord Chem Rev 149:347–365

2. He XM, Carter DC (1992) Atomic structure and chemistry of human serum albumin. Nature 358:209–215

3. Kandagal PB, Ashoka S, Seetharamappa J (2006) Study of the interaction of an anticancer drug with human and bovine serum albumin: spectroscopic approach. J Pharm Biomed Anal 41:393–399

4. Hu YJ, Liu Y, Pi ZB, Qu SS (2005) Interaction of cromolyn sodium with human serum albumin: a fluorescence quenching study. Bioorg Med Chem 13:6609–6614

5. Zhang YZ, Zhou B, Liu YX, Zhou CX, Ding XL, Liu Y (2008) Fluorescence study on the interaction of bovine serum albumin with P-Aminoazobenzene. J Fluoresc 18:109–118

6. Alarcon E, Edwards AM, Aspee A, Moran FE, Borsarelli CD, Lissi EA, Gonzalez-Nilo D, Poblete H, Scaiano JC (2010) Photophysics and photochemistry of dyes bound to human serum albumin are determined by the dye localization. Photochem Photobiol Sci 9:93–102

7. Xiao Q, Huang S, Liu Y, Tian FF, Zhu JC (2009) Thermodynamics, conformation and active sites of the binding of Zn–Nd hetero-bimetallic schiff base to bovine serum albumin. J Fluoresc 19:317–326

8. Hu YJ, Ou-Yang Y, Dai CM, Liu Y, Xiao XH (2010) Site-selective binding of human serum albumin by palmatine: spectroscopic approach. Biomacromolecules 11:106–112

9. Hu YJ, Liu Y, Wang J, Xiao X, Qu SS (2004) Study of the interaction between monoammonium glycyrrhizinate and bovine serum albumin. J Pharm Biomed Anal 36:915–919

10. Hou HN, Qi ZD, OuYang YW, Liao FL, Zhang Y, Liu Y (2008) Studies on interaction between vitamin B12 and human serum albumin. J Pharm Biomed Anal 47:134–139

11. Mei P, Zhang YZ, Zhang XP, Yan CX, Zhang H, Liu Y (2008) Spectroscopic investigation of the interaction between copper (II) 2-oxo-propionic acid salicyloyl hydrazone complex and bovine serum albumin. Biol Trace Elem Res 124:269–282

12. Qi ZD, Zhang Y, Liao FL, OuYang YW, Liu Y, Yang X (2008) Probing the binding of morin to human serum albumin by optical spectroscopy. J Pharm Biomed Anal 46:699–706

13. Qi ZD, Zhou B, Xiao Q, Shi C, Liu Y, Dai J (2008) Interaction of rofecoxib with human serum albumin: determination of binding constants and the binding site by spectroscopic methods. J Photoch Photobio A 193:81–88

14. Zhang YZ, Dai J, Liu C, Zhang XP, Ding XL, Liu Y (2008) Interaction of N'-(1-carboxyethylidene) salicylhydrazide with bovine serum albumin. Chinese J Chem 26:1023–1029

15. Zhang YZ, Chen XX, Dai J, Zhang XP, Liu YX, Liu Y (2008) Spectroscopic studies on the interaction of lanthanum(III) 2-oxo-propionic acid salicyloyl hydrazone complex with bovine serum albumin. Luminescence 23:150–156

16. Cheng XX, Liu Y, Zhou B, Xiao XH, Liu Y (2009) Probing the binding sites and the effect of berbamine on the structure of bovine serum albumin. Spectrochim Acta A 72:922–928

17. Zhang YZ, Dai J, Xiang X, Li WW, Liu Y (2010) Studies on the interaction between benzidine and bovine serum albumin by spectroscopic methods. Mol Biol Rep 37:1541–1549

18. Hu YJ, Liu Y, Sun TQ, Bai AM, Lu JQ, Pi ZB (2006) Binding of anti-inflammatory drug cromolyn sodium to bovine serum albumin. Int J Biol Macromol 39:280–285

19. Han XL, Mei P, Liu Y, Xiao Q, Jiang FL, Li R (2009) Binding interaction of quinclorac with bovine serum albumin: a biophysical study. Spectrochim Acta A 74:781–787

20. Hu YJ, Yu HG, Dong JX, Yang X, Liu Y (2006) Spectroscopic studies on the interaction between 3, 4, 5-trimethoxybenzoic acid and bovine serum albumin. Spectrochim Acta A 65:987–991

21. Hu YJ, Liu Y, Shen XS, Fang XY, Qu SS (2005) Studies on the interaction between 1-hexylcarbamoyl-5-fluorouracil and bovine serum albumin. J Mol Struct 738:143–147

22. Hu YJ, Liu Y, Zhang LX, Zhao RM, Qu SS (2005) Studies of interaction between colchicine and bovine serum albumin by fluorescence quenching method. J Mol Struct 750:174–178

23. Zhang YZ, Zhou B, Zhang XP, Huang P, Li CH, Liu Y (2009) Interaction of malachite green with bovine serum albumin: determination of the binding mechanism and binding site by spectroscopic methods. J Hazard Mater 163:1345–1352

24. Zhang YZ, Dai J, Liu C, Zhang XP, Yang X, Liu Y (2008) Studies of the interaction between Sudan I and bovine serum albumin by spectroscopic methods. J Mol Struct 888:152–159

25. Zhang YZ, Xiang X, Mei P, Dai J, Zhang LL, Liu Y (2009) Spectroscopic studies on the interaction of congo red with bovine serum albumin. Spectrochim Acta A 72:907–914

26. Hu YJ, Liu Y, Zhao RM, Dong JX, Qu SS (2006) Spectroscopic studies on the interaction between methylene blue and bovine serum albumin. J Photoch Photobio A 179:324–329

27. Xiao Q, Huang S, Qi ZD, Zhou B, He ZK, Liu Y (2008) Conformation, thermodynamics and stoichiometry of HSA adsorbed to colloidal CdSe/ZnS quantum dots. Biochim Biophys Acta 1784:1020–1027

28. Dai J, Li CL, Zhang YZ, Xiao Q, Lei KL, Liu Y (2008) Effect of La³⁺ on heat production by mitochondria isolated from hybrid rice. Thermochim Acta 470:77–82

29. Dai J, Liu Y, Zhu JC, Zhang YZ (2006) Microcalorimetric study on the effect of sodium arsenite on metabolic activity of mitochondria isolated from Carassius auratus liver tissue. Chin J Chem 24:997–1000

30. Skulachev VP (1998) Uncoupling: new approaches to an old problem of bioenergetics. Biochim Biophys Acta 1363:100–124

31. Lim HW, Lim HY, Wong KP (2009) Uncoupling of oxidative phosphorylation by curcumin: implication of its cellular mechanism of action. Biochem Biophys Res Commun 389:187–192

32. McLaughlin S (1972) The mechanism of action of DNP on phospholipid bilayer membranes. J Membr Biol 9:361–372

33. Wallace KB, Starkov AA (2000) Mitochondrial targets of drug toxicity. Annu Rev Pharmacol Toxicol 40:353–388

34. Laiho KU, Trump BF (1975) Mitochondrial changes, ion and water shifts in the cellular injury of ehrlich ascites tumor cells. Beitr Pathol 155:237–247

35. Skulachev VP (1997) In: Papa S, Guerrieri F, Tager J (eds) Frontiers of cellular bioenergetics: molecular biology, biochemistry and physiology. Plenum, London

36. Singh RB, Mahanta S, Bagchi A, Guchhait N (2009) Interaction of human serum albumin with charge transfer probe ethyl ester of N,N-dimethylamino naphthyl acrylic acid: an extrinsic fluorescence probe for studying protein micro-environment. Photochem Photobiol Sci 8:101–110

37. Lakowicz JR (1999) Principles of fluorescence spectroscopy, 2nd edn. Plenum, New York, pp 239–240

38. Leckband D (2000) Measuring the forces that control protein interactions. Annu Rev Biophys Biomol Struct 29:1–26
39. Ross PD, Subramanian S (1981) Thermodynamics of protein association reactions: forces contributing to stability. Biochemistry 20:3096–3102
40. Klotz IM, Urquhart JM (1949) The binding of organic ions by proteins, effect of temperature. J Am Chem Soc 71:847–851
41. Kragh-Hansen U (1981) Molecular aspects of ligand binding to serum albumin. Pharmacol Rev 33:17–53
42. Shcharbin D, Janicka M, Wasiak M (2007) Serum albumins have five sites for binding of cationic dendrimers. Biochim Biophys Acta 1774:946–951
43. Kang J, Liu Y, Xie MX, Li S, Jiang M, Wang YD (2004) Interaction of human serum albumin with chlorogenic acid and ferulic acid. Biochim Biophys Acta 1674:205–214
44. Sudlow G, Birkett DJ, Wade DN (1976) Further characterization of specific drug binding sites on human serum albumin. Mol Pharmacol 12:1052–1061
45. Cooper A (1999) Thermodynamic analysis of biomolecular interactions. Curr Opin Chem Biol 3:557–563
46. Frazier RA, Papadopoulou A, Green RJ (2006) Isothermal titration calorimetry study of epicatechin binding to serum albumin. J Pharm Biomed Anal 41:1602–1605
47. Chekmeneva E, Diaz-Cruz JM, Arino C, Esteban M (2009) Binding of Hg^{2+} with phytochelatins: study by differential pulse voltammetry on rotating au-disk electrode, electrospray ionization mass-spectrometry, and isothermal titration calorimetry. Environ Sci Technol 43:7010–7015
48. Turnbill WB, Daranas AH (2003) On the value of c: can low affinity systems be studied by isothermal titration calorimetry? J Am Chem Soc 125:14859–14866
49. Förster T (1965) In: Sinanoglu O (ed) Delocalized excitation and excitation transfer, modern quantum chemistry, vol. 3. Academic, New York, pp 93–137
50. Cyril L, Earl JK, Sperry WM (1961) Biochemists' handbook. E. &F. N. Spon, London
51. Valeur B (2001) Molecular fluorescence: principles and applications. Wiley, New York
52. Abert WC, Gregory WM, Allan GS (1993) The binding interaction of coomassie blue with proteins. Anal Biochem 213:407–413
53. Miller JN (1979) Recent advances in molecular luminescence analysis. Proc Anal Div Chem Soc 16:203–208
54. Charbonneau DM, Tajmir-Riahi H (2010) Study on the interaction of cationic lipids with bovine serum albumin. J Phys Chem B 114:1148–1155
55. Lu ZX, Cui T, Shi QL (1987) Application of circular dichroism and optical rotatory dispersion in molecular biology, 1st edn. Science, Beijing, pp 79–82
56. Sreerama N, Woody RW (1993) A self-consistent method for the analysis of protein secondary structure from circular dichroism. Anal Biochem 209:32–44
57. Whitmore L, Wallace BA (2004) DICHROWEB, an online server for protein secondary structure analyses from circular dichroism spectroscopic data. Nucleic Acids Res 32:W668–W673
58. Cui FL, Fan J, Hu ZD (2004) Interactions between 1-benzoyl-4-p-chlorophenyl thio-semicarbazide and serum albumin: investigation by fluorescence spectroscopy. Bioorg Med Chem 12:151–157
59. Bhattacharya B, Nakka S, Guruprasad L, Samanta A (2009) Interaction of bovine serum albumin with dipolar molecules: fluorescence and molecular docking studies. J Phys Chem B 113:2143–2150